Low-Affinity Platelet Factor 4 ^{1}H NMR Derived Aggregate Equilibria Indicate a Physiologic Preference for Monomers over Dimers and Tetramers†

Kevin H. Mayo

Department of Chemistry and The Fels Institute for Cancer Research and Molecular Biology, Temple University, Philadelphia, Pennsylvania 19122

Received May 21, 1990; Revised Manuscript Received September 12, 1990

ABSTRACT: Low-affinity platelet factor 4 (LA-PF4), unlike another related, sequentially homologous (about 50%) platelet-specific protein, platelet factor 4 (PF4), is an active mitogenic and chemotactic agent. PF4 exhibits a high binding affinity for heparin, while LA-PF4 does not. Both PF4 and LA-PF4 can exist in dimer and tetramer aggregate states. Equilibrium constants for PF4 aggregation have recently been estimated from fractional populations derived from proton nuclear magnetic resonance (NMR) integrals assigned to resonances in monomer, dimer, and tetramer states [Mayo & Chen (1989) *Biochemistry 28*, 9469]. On a 500-MHz NMR time scale, relatively slow exchange among LA-PF4 aggregate species has also allowed Tyr 15 ring proton resonances to be assigned for monomer, dimer, and tetramer states in LA-PF4. As a function of pH and ionic strength, equilibrium association constants for LA-PF4 dimer (K_D) and tetramer (K_T) formation have been estimated from Tyr 15 ring proton resonance integrals. At low ionic strength, K_D reaches a minimum value of 12 M^{-1} at pH 3 where K_T is at its maximum value of 1.6×10^5 M^{-1}. At pH 4.1, K_D and K_T have the same value, 1.1×10^3 M^{-1}, which is the minimum value for K_T. K_D plateaus off to its maximum value of 2.2×10^4 M^{-1} by pH 5.5. These values are significantly lower than those for PF4. Analysis of the pH dependence of K_D and K_T suggests that electrostatic interactions probably among Glu/Asp and Lys/Arg side chains form the predominant force in the monomer–monomer binding process, i.e., K_D, while like-charge repulsion due to proximal, intersubunit Glu/Asp residues decreases K_T as the pH is raised. At pH 7 and low ionic strength, the dimer state is highly favored over the tetramer state. Elevating the solvent ionic strength at pH 7 destabilizes the dimer state. Under these more physiologic conditions, i.e., pH 7 and 0.1–0.2 M NaCl, LA-PF4 monomers are highly favored over dimers and tetramers. For PF4 under similar solvent conditions, tetramers predominate. Differences in biological activities between these homologous platelet-specific proteins may be the result, at least in part, of differing aggregation properties. The biologically active state for PF4 is tetramer, while for LA-PF4 it is monomer. Quaternary structure may, therefore, account for strong heparin binding in PF4, most likely by presenting a more favorable structural matrix for effective glycosaminoglycan interactions.

Low-affinity platelet factor 4 (LA-PF4)[1] belongs to a set of immunologically identical platelet-specific proteins related as N-terminal cleavage products; the others in this set are β-thromboglobulin (βTG) and platelet basic protein (PBP). LA-PF4 is composed of 85 amino acid residues (Niewiarowski et al., 1980; Holt & Niewiarowski, 1980). The amino acid sequences of βTG and PBP are identical with that of LA-PF4 with the exception of N-terminal residues. PBP contains nine additional N-terminal residues (Holt et al., 1986), and βTG has four fewer residues than LA-PF4 (Begg et al., 1978). PBP is thought to be originally synthesized in megakaryocytes and then degraded to LA-PF4 during the maturation of megakaryocytes and platelets. The "low-affinity" in the name LA-PF4 refers to a low affinity for heparin binding as compared with the related platelet-specific protein, platelet factor 4 (PF4). LA-PF4 and PF4 show about 50% sequence homology. PF4 is known to form tetramers under physiological conditions (Moore et al., 1975; Moore & Pepper, 1976; Mayo & Chen, 1989), while aggregation properties in LA-PF4 have not been investigated. Recently, St. Charles et al. (1989) deduced the X-ray crystal structure of des(1–13) bovine PF4, which consists of three strands of antiparallel β-sheet and a C-terminal α-helix with monomer subunits associated in a tetramer, interacting via H-bonded antiparallel β-sheets, salt bridges, and hydrophobic forces. Given its approximate 50% sequence homology with PF4, LA-PF4 may possess similar structural features.

Recent evidence indicates that the anti-heparin effect of PF4 may be its primary physiological function by interacting with cell-surface heparin-like glycosaminoglycans that would otherwise normally promote anticoagulant activity via acceleration of thrombin–antithrombin III complex formation (Marcum & Rosenberg, 1984; Stern et al., 1985). PF4 does appear to bind to vascular sites on endothelial cells in vitro (Busch et al., 1980) and in vivo (Rao et al., 1983). In contrast, it seems likely that the primary physiological function for LA-PF4 may lie elsewhere in mitogenic and chemotactic activities. Caster et al. (1983) reported that connective tissue activating peptide III (CTAP III), which is sequentially identical with LA-PF4, expresses a significant mitogenic activity with respect to connective tissue fibroblasts. More recently, Mullenback (1986) described the mitogenic activity of DNA-recombinant CTAP III. Paul et al. (1980) found that PBP was mitogenic

† This work was supported by grants from the American Heart Association, Southeast Pennsylvania (Phildelphia) Section, and the National Heart, Lung, and Blood Institute (HL-43194) and benefited from NMR facilities made available to Temple University through Grant RR-04040 from the National Institutes of Health.

[1] Abbreviations: LA-PF4, low-affinity platelet factor 4; PF4, platelet factor 4; βTG, β-thromboglobulin; PBP, platelet basic protein; IL-8, interleukin 8; NMR, nuclear magnetic resonance; 2D NMR, two-dimensional NMR spectroscopy; NOESY, 2D NMR nuclear Overhauser effect spectroscopy; NOE, nuclear Overhauser effect; rf, radio frequency; FID, free induction decay; ST, saturation transfer; HPLC, high-performance liquid chromatography.

0006-2960/91/0430-925$02.50/0

for mouse 3T3 fibroblasts. In a comparison of secreted α-granule proteins with regard to their chemotactic activity for fibroblasts, βTG was found to be the most potent (Senior et al., 1983), with activity being expressed at picomolar concentrations.

Questions regarding the quaternary structure and stability of LA-PF4 and PF4 aggregates in solution are important to understanding their mechanisms of action within their peptide family and in relation to heparin binding. Aggregation of PF4 was recently studied by ^{1}H NMR spectroscopy through which resonance assignments could be made for the three aromatic residues, i.e., His 23, His 35, and Tyr 60, in PF4 monomer, dimer, and tetramer states (Mayo & Chen, 1989). Since Tyr 60 (3,5) ring proton resonances were well resolved from state to state, estimation of fractional populations in each state was possible; this then allowed equilibrium association constants for dimer (K_D) and tetramer (K_T) formation to be estimated as a function of pH and ionic strength. With the same approach in this present study, NMR spectroscopic techniques are used to study the mode of association, the relative strength of monomer (dimer) associations, and the nature of subunit interactions for human LA-PF4 in solution. These data are discussed in relation to those for human PF4 (Mayo & Chen, 1989).

Materials and Methods

Isolation of LA-PF4 and PF4. Human blood was collected in acid citrate dextrose in the commercial blood bank. Within 2–5 h after collection of the blood, platelets were washed in Tyrode's solution containing 35% bovine serum albumin according to the technique described by Mustard et al. (1972). The final suspension usually contained (4–8) × 10^9 platelets/mL. Alternately, concentrates of outdated platelets supplied by the American Red Cross were used and processed as described above. Washed platelets were then aggregated by addition of 2 units/mL bovine thrombin at 37 °C for 15 min. Aggregated platelets were removed by centrifugation, and the supernate was incubated at 56 °C for 30 min to inactivate thrombin and to remove fibrinogen. LA-PF4 was then isolated by use of a salt gradient from a heparin–agarose column as described by Rucinski et al. (1979). The LA-PF4 fraction was then desalted by dialysis (0.2% trifluoroacetic acid). The resulting solution was concentrated by lyophilization and further purified by reversed-phase HPLC to yield pure LA-PF4, which was eluted at 34% acetonitrile from a linear H_2O (0.2% TFA)/acetonitrile (0.25% TFA) gradient. Crude LA-PF4 was also purchased from Bioprocessing Ltd., Durham, England.

For PF4, outdated human platelets were obtained from the Red Cross and centrifuged at 10000*g* for 1 h to obtain platelet-poor plasma. This preparation was applied to a heparin–agarose (Sigma) column (bed volume, 50 mL); the column was washed with 0.2, 0.5, 1, and 1.5 M NaCl. The fraction eluting at 1.5 M NaCl, which yielded most of the PF4 (Rucinski et al., 1979), was then desalted by dialysis (0.2% trifluoroacetic acid). The resulting solution was concentrated by lyophilization. From about 50 units of outdated platelets, 20 mg of PF4 generally resulted.

Protein Concentration. Protein concentration was determined by the method of Lowry et al. (1951), and results were calculated from a standard dilution curve of human serum albumin. An alternative method used to determine PF4 concentration was that of Waddell (1956).

Nuclear Magnetic Resonance (NMR) Spectroscopy. Samples for ^{1}H NMR measurements had been lyophilized and redissolved in ^2H_2O immediately before the experiment. The final protein concentration ranged from 0.5 to 20 mg/mL as indicated in the text. The p^{2}H was adjusted by adding microliter increments of NaO^{2}H or ^{2}HCl to a 0.6-mL sample. All measurements were done at the p^{2}H value indicated in the text, read directly from the pH meter, and not adjusted for isotope effects.

^{1}H NMR spectra were recorded in the Fourier mode on a GE GN-omega 500 spectrometer (500 MHz for protons). The solvent deuterium signal was used as a field-frequency lock. All chemical shifts are quoted in parts per million (ppm) downfield from sodium 4,4-dimethyl-4-silapentane-1-sulfonate (DSS).

Two-dimensional NOESY (Jeener et al., 1979) NMR spectra (mixing time of 0.2 s) were accumulated in ^2H_2O as 512 time incremented, 1024-point spectra in the phase-sensitive mode (States et al., 1982). Data processing was done on a Sun −3/160 computer with software supplied by GE on the spectrometer. FIDs were first multiplied by a Lorentzian/Gaussian transformation or shifted sine-bell function, and data sets were zero-filled to 1024 in the evolution dimension.

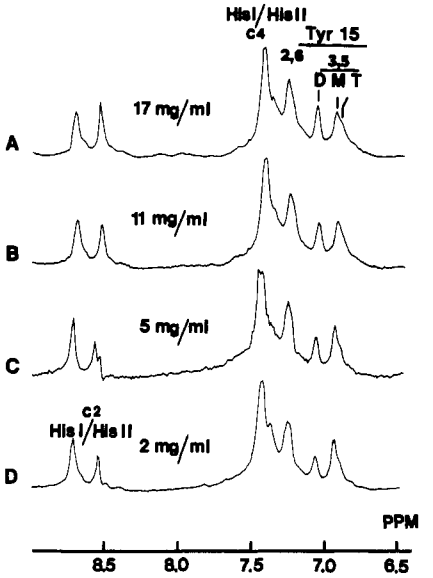

FIGURE 1: Proton NMR spectra of LA-PF4. 500-MHz proton NMR spectra of human LA-PF4 are shown. Lyophilized protein samples were dissolved in ^2H_2O, pH 4.2 and 303 K, containing LA-PF4 concentrations as listed in the figure. No buffer or salt was added to these solutions. The resonance label prefixed M, D, and T stand for monomer, dimer, and tetramer states, respectively.

Results

Not unlike human PF4 (Mayo & Chen, 1989), LA-PF4 demonstrates concentration-dependent proton NMR spectral intensity changes. Figure 1A shows the aromatic region of a spectrum taken with a relatively high LA-PF4 concentration of 17 mg/mL, while Figure 1B–D shows spectra taken with decreasing protein concentrations as labeled in the figure. Aggregation is the most likely explanation for these concentration-dependent spectral changes. Similar NMR spectral changes have been observed for homologous PF4 (Mayo & Chen, 1989).

A 2D NMR NOESY contour plot of the aromatic region (Figure 2) allows identification and grouping of three sets of tyrosine (3,5) and (2,6) ring proton resonances. As is normally observed, the more shielded resonance in each set has been assigned as the (3,5) resonance (Wüthrich, 1986). The most upfield resonance in Figure 1 is comprised of overlapping tyrosine (3,5) resonances in two states. Another Tyr 15 (3,5) resonance neighbors it at 6.94 ppm. Other non-tyrosine res-

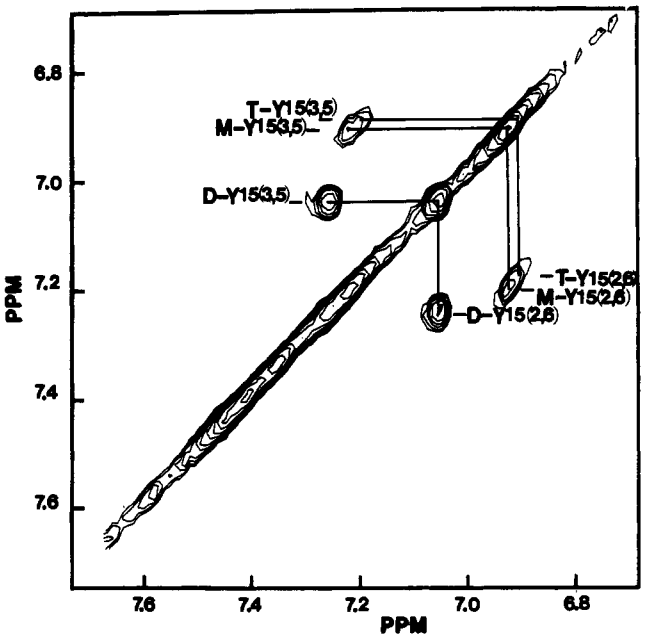

FIGURE 2: NOESY contour plot. The aromatic resonance region of a NOESY contour plot of LA-PF4 at pH 4.2 and 303 K is shown. The mixing time was 0.2 s, and other experimental details are described under Materials and Methods.

onances in Figure 1 must be due to His 30 and His 45 C2 and C4 ring proton resonances. We have focused our attention on Tyr 15, His 30, and His 45 side-chain resonances since these are simplest to resolve, assign, and discuss. His 30 and His 45 have been labeled as His I and His II since sequence-specific resonance assignments are presently unknown.

Having assigned and grouped tyrosine ring proton resonances, we can return to Figure 1. Note that, at the lowest protein concentration, the second most upfield tyrosine (3,5) resonance group is the most intense. Although not clear in Figure 1, this resonance also exhibits the narrowest half-height line width of 15 Hz as estimated from line-shape analysis. Even at this concentration, however, a slightly more upfield shifted, broader tyrosine (3,5) resonance, i.e., 40-Hz half-height line width, overlaps the narrower one. As the concentration is increased, the narrower resonance decreases in intensity while the broader one increases. The most downfield Tyr 15 (3,5) resonance also increases in intensity; its line width is about 20 Hz, lying between the values of the other two. These observations suggest tentative assignment of aggregate states labeled in Figures 1 and 2 as monomer (M), dimer (D), and tetramer (T). The most upfield, broadest tyrosine (3,5) resonance is due to tyrosine in the tetramer state, while the narrowest overlapping one is due to that in the monomer state and the remaining one with an intermediate line width is due to that in the dimer state.

Confirmation of these aggregate state assignments comes from the following analysis of fractional populations in each presumed state according to the general association equilibrium equation. Since the total area under all Tyr 15 (3,5) ring proton resonances remains constant, an estimate of the mole fraction for each state can be had, and by knowing the total protein concentration in terms of moles of Tyr 15, one can estimate the LA-PF4 equilibrium concentration in each state.

Resonance areas were estimated by Gaussian/Lorentzian line-shape fitting to NMR data like that shown in Figure 1. Given the fact that monomer and tetramer Tyr 15 (3,5) resonances overlap and that a curvilinear base line is apparent, Figure 3 gives an example of the general line-shape fitting procedure used for spectral analyses in this paper. First, a

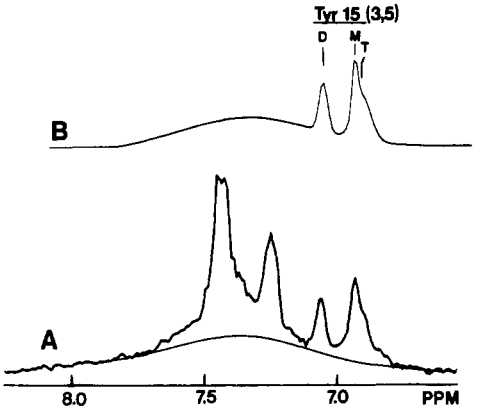

FIGURE 3: Line-fitting procedure for Tyr 15 (3,5) resonance areas. An example of the Gaussian/Lorentzian line-fitting procedure is shown for the Tyr 15 (3,5) proton resonance region from one NMR spectrum. The base line was first approximated with a broad Gaussian line (A); additional lines were then added to estimate aggregate areas as described in the text. The sum of all superimposed lines is shown in (B).

broad Gaussian line was fit to approximate the curvilinear base line under the His I and II C4 and Tyr 15 (2,6) and (3,5) resonances (Figure 3A). The specific origin of this rather broad resonance component is unknown; while it could reflect the presence of higher than tetramer aggregate species, the extent of this effect varied randomly from sample to sample. Some samples demonstrated a relatively flat base line as will be seen later. Once the base line was corrected in this way, additional Gassian/Lorentzian lines were then fit to Tyr 15 (3,5) resonances in each aggregate state. Variations in the area of this broad component among similar LA-PF4 samples did not affect the results described below. Dimer resonance fits were easiest since spectral overlap was not a problem. For deconvolution of overlapping monomer and tetramer Tyr 15 (3,5) resonances, two superimposed Gaussian lines were used. Initially, chemical shifts and line widths for these were taken for the monomer resonance acquired at low LA-PF4 concentration and low pH, where greater than 90% monomer state exists; for the tetramer resonance, a higher protein concentration and higher pH were used, where the tetramer state predominates. Initial resonance heights were then estimated from the position of the upfield tetramer shoulder. For the most part, only resonance heights had to be significantly adjusted in order to obtain the best fit. Figure 3B shows an example of summed Gaussian lines for monomer, dimer, and tetramer resonances. This can be compared to the actual NMR spectral region in Figure 3A. For NMR data sets described herein, this procedure was carried out on two different protein samples. Derived areas from these fits varied at most by about 20%, less so for dimer resonance fits. Partly for this reason, calculated equilibrium constants given in later figures are shown as their natural logarithms, where variations appear smaller. A 20% difference or so in area estimates from one sample to another will produce only a 0.2 change in the natural logarithm.

On the basis of general considerations of monomer, dimer, and tetramer equilibria, the Hill equation can be written as

$$\ln [M_n] = n \ln [M] + \ln K \qquad (1)$$

where M stands for monomer (dimer) and n is the stoichiometric coefficient; the symbol M_n stands for the aggregation state (dimer or tetramer as the case may be). The brackets refer to concentration. If we plot ln $[M_n]$ versus ln [M] at a pH value of 4.2 (Figure 4) where M_n is identified with the Tyr 15 (3,5) dimer resonance and M is taken to be the mo-

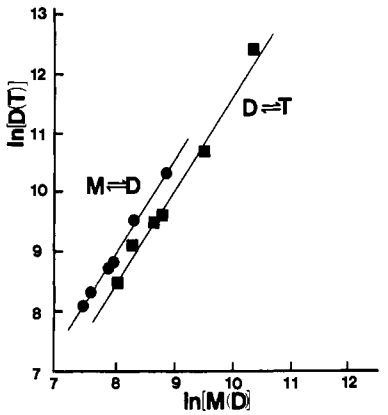

FIGURE 4: Hill plots for dimer and tetramer formation. Fractional populations for monomers (M), dimers (D), and tetramers (T) were extracted from the NMR data as a function of LA-PF4 concentration as described in the text. The natural logarithm of the presumed tetramer (or dimer) concentration was plotted versus that of the dimer (or monomer) concentration to yield a slope that gave the number of associating subunits according to eq 1. The solid lines represent least-squares fits of the data.

nomer resonance, we arrive at a value for n of 1.8, which indicates that two subunits are associating to yield dimers. If one now makes a similar plot where the assumed "dimer" resonance is taken as M and the "tetramer" as M_n in eq 1 and ln $[M_n]$ is plotted versus ln [M], we derive a slope, n, of 1.7. These data confirm the assignment of Tyr 15 (3,5) proton resonances in monomer, dimer, and tetramer states and provide evidence for the normally observed bimolecular mechanism of association going from monomers to dimers and then from dimers to tetramers.

Equilibrium constants for association are given as

$$K_D = [D]/[M]^2 \qquad K_T = [T]/[D]^2 \qquad (2)$$

Knowing the mole fraction of M, D, and T derived from resonance integrals (Gaussian/Lorentzian line-shape fitting to data) and the total protein concentration per mole of Tyr 15 allows one to estimate equilibrium association constants K_D and K_T from data like those shown in Figure 5. Figure 5 presents representative spectra for LA-PF4 as a function of pH. Tyr 15 ring proton resonances are not chemically shifted by pH variations. Figure 6A gives a plot of ln K_D and ln K_T versus the solution pH for pH values where it was possible to estimate mole fractions for monomer, dimer, and tetramer. In cases where only monomer and tetramer populations could be estimated, i.e., low pH, the overall association equilibrium constant K_{DT} is shown (Figure 6B); this is equal to $K_T \times K_D^2$. At about pH 4, K_T and K_D approach the same value. As the pH is raised, K_T falls where K_D increases. As the pH is raised to values above about pH 5, K_T remains constant and K_D seems to plateau out. Above pH 5, dimers are favored over tetramers by about 2 to 1. For comparison, K_D, K_T, and K_{DT} values for PF4 (Mayo & Chen, 1989) are also shown in this plot as open symbols. Lines drawn through data points are discussed in the next section.

The pH dependence of protein aggregation could be the result of several factors related to the nature of monomer–monomer and dimer–dimer interactions. Two types of charge interactions could cause association to increase with decreasing pH as is the case with dimer–dimer associations: (1) if there were a pair of interacting carboxyls, protonation of one would eliminate the unfavorable (repulsive) electrostatic interaction; (2) protonation of a neutral side chain, with the creation of a positive charge, could result in a favorable interaction with a negatively charged side chain. Decrease in association with

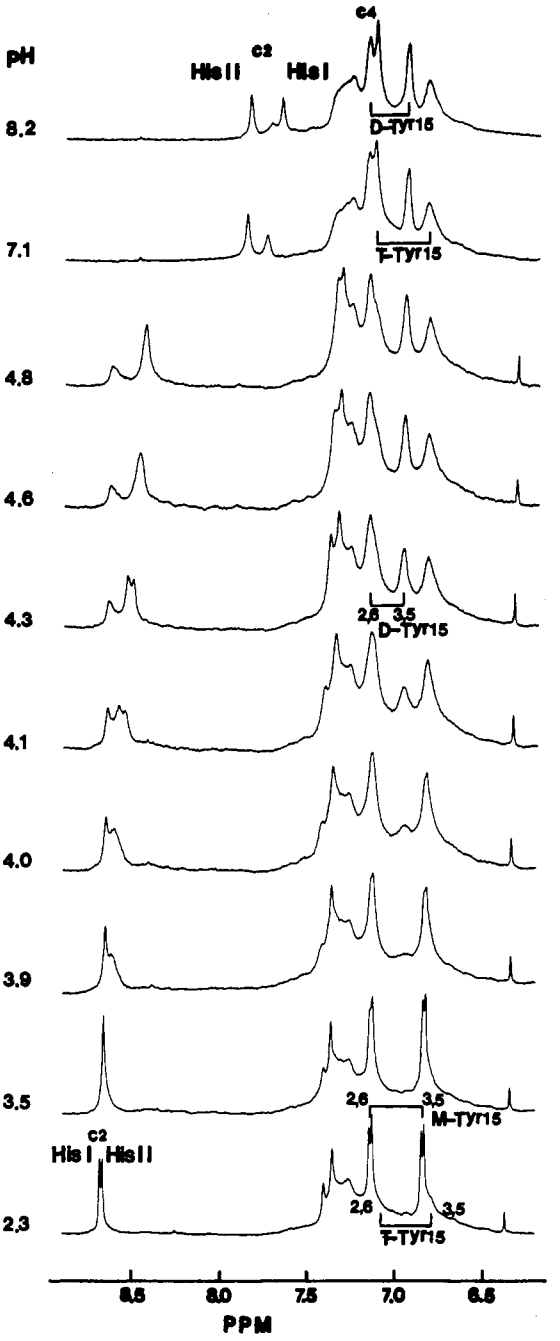

FIGURE 5: Effect of pH on LA-PF4 aromatic proton resonances. A series of proton NMR spectra taken in ^2H_2O are shown for the LA-PF4 aromatic resonance region as a function of the solution pH as indicated in the figure next to each spectrum. The LA-PF4 concentration was 4 mg/mL. The temperature was 303 K. The resonance label prefixes M, D, and T stand for monomer, dimer, and tetramer states, respectively.

decreasing pH could be accounted for by (1) the elimination of an attractive cationic–anionic interaction by the protonation of the anionic group or (2) the increasing unfavorable long-range electrostatic repulsion between two macroions with a net positive charge. Alternatively, pH-induced conformational transitions could be occurring. It is unlikely, however, that gross conformational changes are occurring under the conditions studied for several reasons: (1) we are dealing with a narrow pH range; (2) two disulfide bridges that impose structural constraints on LA-PF4 are not modified by these pH changes; (3) at low pH values, tetramer association is enhanced while dimer association is attenuated, suggesting that protein denaturation, at least down to pH 2, is not occurring.

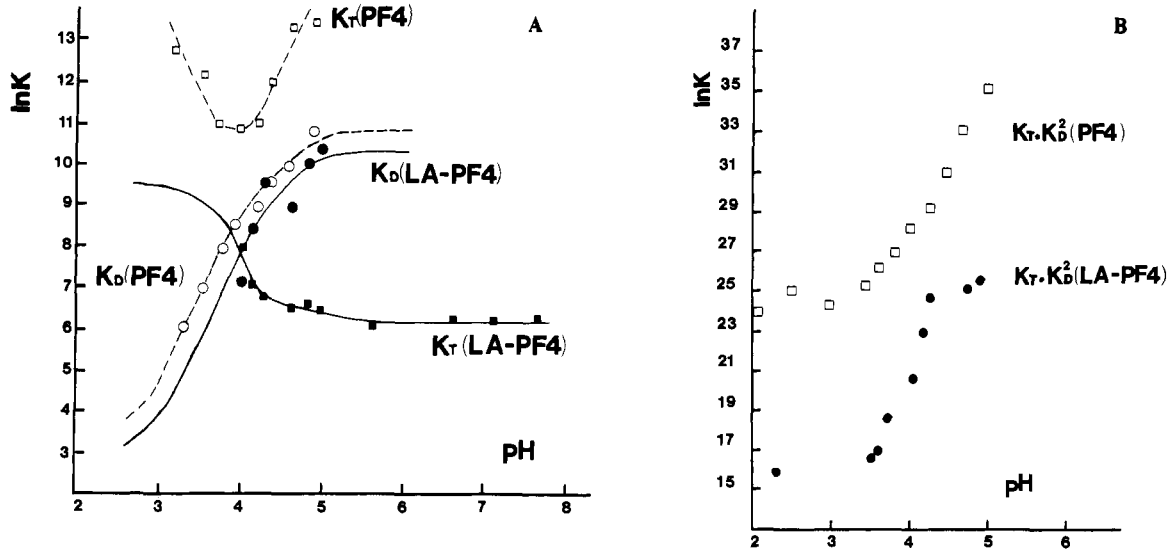

FIGURE 6: Effect of pH on equilibrium constants for LA-PF4 and PF4. Plots are shown for LA-PF4 association equilibrium constants as ln K_T and ln K_D versus pH (A). Values for K_T and K_D were derived as discussed in the text. The overall equilibrium constant for LA-PF4 subunit association, K_{DT} ($=K_T \times K_D^2$), is also given (B). For comparison, equilibrium constants for PF4 as estimated by Mayo and Chen (1989) are shown with open symbols and dashed lines. The solid line through K_D values represents the best fit of the data to eq 6. The solid line through K_T values (for LA-PF4 only) was fit to the Henderson–Hasselbalch titration equation; part of the K_T estimates were calculated from K_{DT} values and the completed function of K_D versus pH.

Assuming that conformational changes, if they do occur, are minimal, one can analyze the pH dependence on association to a first approximation in terms of interactions between ionizable groups fixed in space. This type of analysis was used for the study of α-chymotrypsin dimerization (Aune et al., 1971; Aune & Timasheff, 1971) and PF4 dimerization and tetramerization (Mayo & Chen, 1989). This approach is based on the ligand activity relationships developed by Wyman (1964). Since the slope of ln K versus pH in Figure 6A is about 4 for dimer association, the simplest explanation is to assume that four groups are involved in the interaction (Mayo & Chen, 1989). This value is plausible since 2-fold symmetry axes are suggested to exist between dimer pairs by comparison to tetramer bovine PF4 (St. Charles et al., 1989). This would mean that an interacting charge group on one monomer subunit is symmetry related to the same group on an opposing monomer subunit. In other words, we are probably dealing only with two different side chains in these interactions.

The pH dependence of the association (dimerization) equilibrium constant is given by

$$\ln K = \ln K(\mathrm{pH}=\infty) + 2 \ln \left[\frac{(1 + a_H/K_{1,D})(1 + a_H/K_{2,D})}{(1 + a_H/K_{1,M})(1 + a_H/K_{2,M})} \right] \quad (3)$$

where a_H is essentially given by the hydrogen ion concentration; K_1 and K_2 are the ionization constants for the interacting groups in M and D states, respectively (or D and T states, respectively, as the case may be). The data of Figure 6A were iteratively curve fitted to this expression. In the case of monomer–monomer (dimer) association, a satisfactory fit was attained as shown by the solid line in Figure 6A for K_D (LA-PF4). This yielded values of $pK_{1,M} = 4.6$ and $pK_{2,M} = 8.7$; on dimerization the values changed to $pK_{1,D} = 2.6$ and $pK_{2,D} = 10.3$. The pK_a values of these interacting groups are most readily identified with Glu/Asp and Lys/Arg side-chain ionizations.

The eq 3 fit for monomer–monomer association data shown in Figure 6A indicates that K_D should plateau out at about pH 5.5 and reach a minimum at about pH 2.5. Since we have estimates for K_{DT} ($=K_T \times K_D^2$) down to about pH 2.5, this trend at low pH would suggest that K_T should continue to increase down to about pH 3 and plateau out as shown in Figure 6A. This enhances the difference between K_D and K_T, further explaining why dimer populations were not observed at lower pH values. It should be noted that the values measured for K_{DT} do not impose unique constraints on the values of K_D and K_T, since these extended low pH values are model dependent.

For the dimer–dimer (tetramer) association curve, a fit to eq 3 could not be obtained. Only if two interacting negatively charged groups were considered could this trend be explained. A fit of these data to the Henderson–Hasselbalch equation (Lehninger, 1978) for a standard titration curve gave an estimated pK_a value of 3.9. This is clearly an estimate since only partial data for the titration curve are present; the other part was deduced by back-calculating from K_D and K_{DT} values as mentioned above. Opposing, proximal intersubunit Glu or Asp residues are most likely responsible for this pH effect in dimer–dimer association.

Aggregation apparently has little effect on His II, while it has a significant effect on His I and Tyr 15. Monomer Tyr 15 (3,5) ring proton resonances are downfield shifted by about 0.07 ppm on going to the dimer state, and dimer Tyr 15 (3,5) ring proton resonances are upfield shifted by about 0.08 ppm on going to the tetramer state. These shifts are accompanied by line-width changes; monomer Tyr 15 ring proton resonance line widths are about 15 Hz at half-height, while they are increased to about 40 Hz in the tetramer state. Line-width increases are expected on aggregation, while chemical shift changes are difficult to interpret. State-specific His C2 proton resonances could be assigned in some cases after analysis of concentration- and pH-dependence data where population and chemical shift differences among aggregation states allowed assignment. His C4 proton resonances were generally not as well resolved and have not been considered here. His II C2 proton resonances cannot be resolved for aggregate species. A His II pK_a value of 5.9 can be estimated by using the Henderson–Hasselbalch equation (Lehninger, 1978) and by assuming an overall chemical shift change of 1 ppm between fully protonated and fully unprotonated states. His I C2 proton resonances for aggregate species are resolved at only a few pH

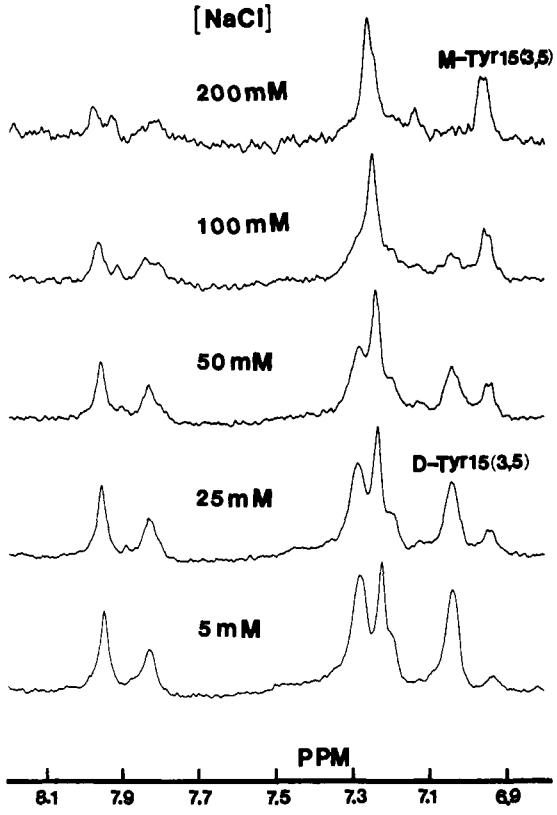

FIGURE 7: Effect of ionic strength. A series of NMR spectra for the aromatic proton resonance region of LA-PF4 are shown as a function of the NaCl concentration as indicated in the figure. The protein concentration was 2 mg/mL at 303 K and pH 4.0 in ^2H_2O.

values, but a rough pK_a estimate for His I is around 5.8.

Effect of Ionic Strength. Since NaCl is used to dissociate LA-PF4 from heparin–agarose and is naturally, physiologically present, it may play a role in LA-PF4 aggregation. Moreover, since LA-PF4 aggregation is pH dependent, electrostatic interactions are probably involved in the association process, and varying the solution ionic strength can be used to further explore this phenomenon. Figure 7 gives a series of NMR spectra at pH 7 and at a fixed LA-PF4 concentration (3 mg/mL) as a function of NaCl concentration. This LA-PF4 concentration was chosen for an initially high dimer population. At low ionic strength, this distribution is apparent in Figure 7. It is unclear whether the more upfield Tyr 15 (3,5) resonance is due to tetramer and/or monomer species. Although the apparent line width reflects that of the tetramer species, exchange broadening at low monomer population cannot be excluded. Addition of 25 mM NaCl shifts the overall equilibrium from dimer (and possibly tetramer) to monomer as indicated by the apparent Tyr 15 (3,5) resonance splitting and apparent decrease in line width more toward the monomer species. On addition of 50 mM salt and above, aggregation equilibria are shifted more in favor of the monomer state. By 200 mM NaCl, most LA-PF4 molecules are found in the monomer state. Estimation of K_D values as a function of NaCl concentration shows this quantitatively in Figure 8. At the lowest ionic strength shown in Figure 7, it was assumed that the more upfield Tyr 15 (3,5) resonance is due to a 10% monomer fractional population in calculating a K_D value; this means that that K_D value is a minimum value. Furthermore, at 200 mM NaCl, the dimer fractional population, if present at all within the noise level, was simply taken to be about 10%; this represents a maximum K_D value at this higher ionic strength. In any event, K_D is decreased at least 400-fold on addition of 200 mM NaCl.

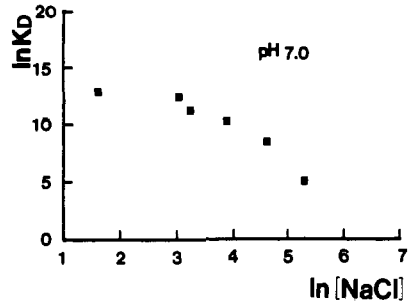

FIGURE 8: Effect of ionic strength on equilibrium constants. The natural logarithm of K_D at pH 4 is plotted versus the natural logarithm of the NaCl concentration. The protein concentration was 2 mg/mL at 303 K at pH 4.

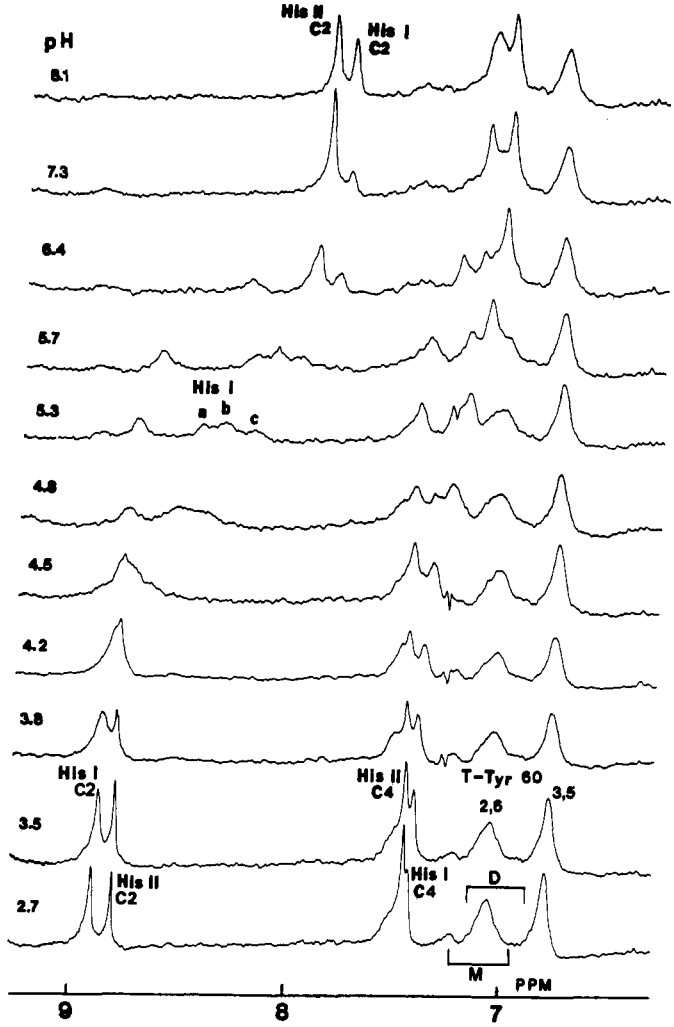

FIGURE 9: ^1H NMR aromatic resonance region of PF4 as a function of pH. 500-MHz ^1H NMR spectra of PF4 show the aromatic ring proton resonance region as a function of pH. The sample concentration was 0.25 mM in 0.2 M NaCl at 303 K. Each spectrum represents the time averaging of 1024 transients; the FID was multiplied by an exponential weighting function to give 2-Hz line broadening.

For comparison to LA-PF4, Figure 9 presents a series of NMR spectra for PF4 in 0.2 M NaCl as a function of pH. Like Tyr 15 in LA-PF4, PF4 Tyr 60 (3,5) proton resonance chemical shift values are pH and salt concentration independent (Mayo & Chen, 1989), but unlike Tyr 15 in LA-PF4, PF4 Tyr 60 (3,5) ring proton resonances in each state are resolved from one another. PF4 Tyr 60 ring proton resonance chemical shift positions as assigned in Mayo and Chen (1989) for monomer (M), dimer (D), and tetramer (T) states are

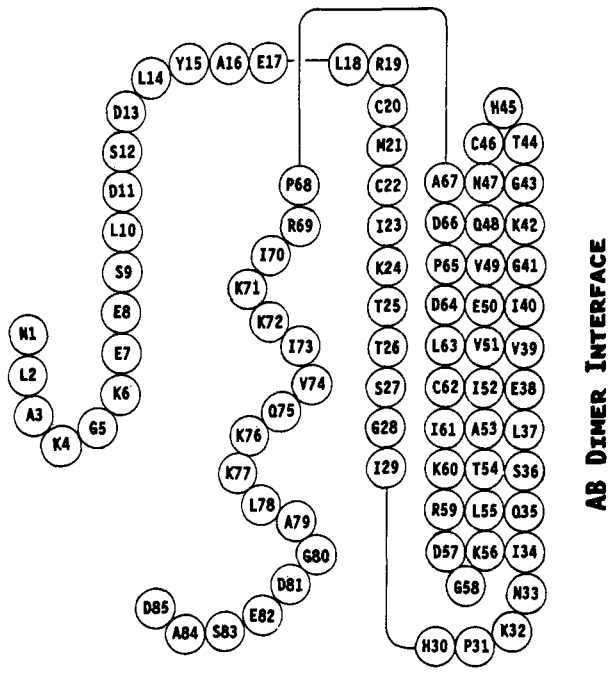

FIGURE 10: Amino acid sequence for human LA-PF4. The amino acid sequence of LA-PF4 is shown. Each circle represents one amino acid residue. The chain is folded to generally represent secondary and tertiary structure elements in homologous bovine PF4 (St. Charles et al., 1989) as discussed in the text.

indicated in Figure 9. At low pH, monomer and dimer species seem to be absent, although a resonance at the M-Tyr 60 (2,6) resonance position is apparent; its (3,5) resonance, however, is not evident. This resonance, therefore, cannot be explained. In any event, tetramer resonance populations dominate at all pH values. At higher pH (7.3 and 8.1), however, it is unclear if a small dimer fraction is present as suggested by the shallower slope on the downfield side of the (3,5) resonance. This unclarity is expounded by the fact that Tyr 60 tetramer line widths are significantly increased at higher pH values in the presence of 0.2 M NaCl, where dimer and tetramer resonance overlap becomes a problem. Line-shape analysis suggests that any dimer population which may be present is less than about 10%. Since at pH 5.3 or 5.7 the dimer resonance is not apparent, it is likely that at higher pH values only the tetramer resonance occurs. This observation is in contrast to the LA-PF4 case, where the monomer state was highly favored at higher pH values in 0.1–0.2 M NaCl.

Discussion

Human LA-PF4 and PF4 are homologous platelet-specific proteins released from platelets by thrombin-stimulated platelet aggregation. The primary physiologic function of PF4 seems to be its potent anti-heparin effect, while LA-PF4 is active as a mitogenic and chemotactic agent. It is known that PF4 can form stable tetramers (Moore et al., 1976; Mayo & Chen, 1989) and dimers (Mayo & Chen, 1989) in solution, and these present NMR data indicate that LA-PF4 can also form dimers and tetramers. The amino acid sequence for LA-PF4 is given in Figure 10 for the ensuing discussion. From knowledge of the X-ray diffraction derived structure of a fragment of bovine PF4 (St. Charles et al., 1989) and conserved amino acid sequence alignments, antiparallel β-sheet and C-terminal α-helix folding patterns are also suggested for LA-PF4 in Figure 10. Since the structurally constraining cystine and β-sheet domain residues are conserved in LA-PF4, one might predict similar backbone structural features. While the truth of this will have to await complete NMR structure analysis of LA-PF4, it is clear that both PF4 and LA-PF4 do share some very similar aggregation properties that support the suggestion of structural conservation. The K_D versus pH curve (Figure 6) for LA-PF4 relative to PF4, for example, is nearly the same, in both shape and position. This can probably be attributed to similar intersubunit contact domain(s) and similar pK_a values for Glu/Lys residues involved in dimer intersubunit salt bridges. The main difference between LA-PF4 and PF4 aggregation lies in dimer–dimer (tetramer) association. Above about pH 5, K_T for LA-PF4 remains constant and is about 4 orders of magnitude smaller than that for PF4 (see Figure 6). At least some critical intersubunit (interdimer) interactions, therefore, differ in PF4 relative to LA-PF4 in order to explain significantly different dimer–dimer (tetramer) association equilibria.

X-ray structure analysis of tetramer bovine PF4 (St. Charles et al., 1989) shows that the crystal arrangement of the four monomer subunits (identified as A, B, C, and D) is such that two types of dimers are formed, i.e., AB(CD) type and AC-(BD) type. This quaternary structural arrangement may be at least partially conserved in human LA-PF4. The present NMR data indicate the presence of one apparent dimer resonance reflected in the Tyr 15 resonance populations, suggesting that one LA-PF4 dimer is thermodynamically favored in solution. Since two different equilibrium association pH trends, one for monomer–monomer association (K_D) and one for dimer–dimer association (K_T), are observed, preference for one dimer type is strongly suggested. If no preference existed, then the effect of pH would be the same, an average of both types. A similar observation was deduced for PF4 dimer preference (Mayo & Chen, 1989). In AC-type dimers of bovine PF4, two salt bridges have been proposed between Glu 43 in one subunit and Lys 65 in the other subunit. No salt bridges were proposed in AB-type dimers. The assumption of structural homology of monomer bovine PF4 with monomer human LA-PF4 would suggest the presence of intersubunit salt bridges between Glu 38 and Lys 60 in LA-PF4 dimers since amino acid sequences in these domains are highly conserved. Tentative identity of the favored solution dimer as the AC type can be made by considering pK_a values of interacting charge groups derived from monomer–monomer (K_D) association equilibrium data (Figure 6; eq 3). The best fit of eq 3 to these data yields dimer state pK_a values of 2.6 and 10.3 for the two interacting groups. The existence of a salt bridge between Glu and Lys residues in LA-PF4 AC-type dimers is consistent with these pK_a values. Similar arguments and assignments of the AC-type dimer were made for human PF4 (Mayo & Chen, 1989).

The pH dependence of K_T also indicates a role for electrostatic interactions in LA-PF4 dimer–dimer (tetramer) association. This pH dependence can be explained by two pairs of interacting, negatively charged residues, i.e., Asp or Glu (one on each monomer). This is the case in tetramer bovine PF4 (St. Charles et al., 1989), where two opposing glutamic acid residues in an intersubunit, antiparallel β-sheet domain are involved in AB(CD) subunit interactions as indicated in Figure 10. The amino acid sequences flanking this glutamic acid residue are highly conserved in LA-PF4, i.e., Glu 38. This supports the proposal of general structural conservation between bovine PF4 and human LA-PF4. Interestingly, AC dimer preference can be explained by considering the situation where Lys/Glu salt bridges involving the opposing glutamic acid residues are absent; in that case, negative charge repulsion above the Glu pK_a value would destabilize AB-type dimers. Only formation of that salt bridge or lowering the pH to below

the Glu pK_a would allow formation of a stable AB dimer. This trend is observed for PF4 tetramer formation (Mayo & Chen, 1989) and here for LA-PF4 where the K_T value is increased as the pH is decreased.

Qualitatively, equilibrium-exchange lifetimes or flux rates for subunit association/dissociation can be derived from these data. Since resonances in all three aggregate states can be observed in NMR spectra for either LA-PF4 or PF4, it is apparent that aggregate states exchange among each other relatively slowly on a 500-MHz NMR time scale; this translates to equilibrium-exchange lifetimes greater than about 10 ms. This is the upper limit for LA-PF4 and PF4 subunit exchange. Since saturation-transfer, or perhaps more precisely magnetization-transfer, cross-peaks were observed among Tyr 60 ring proton resonances in NOESY spectra for PF4 (Mayo & Chen, 1989), a lower exchange limit for PF4 aggregates can also be deduced that must lie on the order of the Tyr 60 ring proton resonance spin–lattice relaxation time of about 0.2–0.5 s. For LA-PF4, NOESY spectra (see Figure 2) show no magnetization-transfer cross-peaks, strongly suggesting that subunit-exchange lifetimes must be considerably longer than the Tyr 15 (3,5) ring proton resonance spin–lattice relaxation time. By comparing PF4 and LA-PF4 association equilibrium constants and assuming the same Stokes–Einstein-based "diffusion-limited" association rate constant of about 1×10^6 M^{-1} s^{-1}, rate constants for tetramer PF4 and LA-PF4 unimolecular dissociation should be about 10 s^{-1} and 1000 s^{-1}, respectively, with a factor of 100 times difference in favor of PF4 tetramers. This would indicate that the PF4 tetramer state is longer lived or more "stable" than the LA-PF4 tetramer state. By the same reasoning, little difference in dimer PF4 and dimer LA-PF4 lifetimes is found to exist, suggesting near equal "stability" of both dimer species.

The question remains open as to why two related, sequentially homologous, platelet-specific proteins have varying biological activities. At least part of the answer probably lies in their having different quaternary structural properties. Under physiologic conditions, i.e., pH 7 and 0.1–0.2 M NaCl, LA-PF4 monomers predominate while PF4 dimers form relatively tightly associated tetramers. In terms of biological activity, this effectively means that, under physiologic conditions at an LA-PF4 blood serum concentration of 20 μg/mL (estimated), LA-PF4 monomers are favored by about 2500:1 over LA-PF4 dimers and tetramers. For PF4 this is difficult to estimate since a distinct K_T value could not be derived due to a preponderence of tetramer population and an unestimatable dimer fractional population. If we assume a greater than 90% tetramer population, which the data do indicate, then a PF4 concentration of 20×10^{-6} M under physiologic conditions would produce a tetramer:dimer population ratio of about 2:1, respectively. This is actually likely to be even greater in favor of the tetramer state. It should be noted that when PF4 is initially released from platelets, the localized PF4 concentration is likely to be in the milligram per milliliter range and would clearly show about a 100:1 tetramer to dimer preference. The biologically active structure for LA-PF4, therefore, is probably a monomer, whereas for PF4, tetramers probably constitute the active state. On a structural level, the reason for this will have to await complete structure elucidation and comparison of both proteins. At present, it is evident that while AC-type dimer contacts seem to be conserved in both proteins, AB-type contacts are different. Differences in their dimer–dimer (tetramer) aggregation equilibria suggest that variances in specific contact domain residues and/or monomer/dimer subunit structural differences are causal. An imperfectly aligned intersubunit, antiparallel β-sheet domain in LA-PF4, for example, could account for this observation.

Cowan et al. (1986) proposed a model for the binding of heparin to tetrameric PF4 on the basis of an analysis of X-ray crystallographic data and suggested that lysine residues at the C-terminal end of PF4 form a region of localized 2-fold symmetry on the C-terminal α-helix. The proposed heparin-binding-domain sequence in PF4, i.e., LYKKIIKKLL (Handin & Cohn, 1976; Lawler, 1981; Loscalzo et al., 1985), is in fact now known to position the lysines above and below each other on the solvent-exposed side of that C-terminal helix (St. Charles et al., 1989). A 16-residue polysaccharide chain is considered necessary to wrap around the PF4 tetramer matrix (Denton et al., 1983; Cowan et al., 1986; Ibel et al., 1986). On the basis of this information, it has been hypothesized that the proposed heparin-binding sequence in PF4, i.e., LYKKIIKKLL, conforms in several proteins to a heparin-binding consensus sequence of the form XBBXBX or XBBBXXBX, where B stands for a basic amino acid residue (Lys/Arg) and X stands for hydropathic amino acid residues (Cardin & Weintraub, 1989). LA-PF4 has a similar cluster of lysine residues at its C-terminal domain. The lower affinity of LA-PF4 for heparin has been suggested (Handin & Cohen, 1975; Lawler, 1981; Loscalzo et al., 1985) to be the result of a C-terminal amino acid sequence difference that, in the presumed LA-PF4 C-terminal α-helix, causes the two pairs of lysine residues to be spatially misaligned by the presence of an additional residue separating the lysines, i.e, RIKKIVQKKLA. This analysis probably assumed a priori that LA-PF4 was in the tetramer state or that the strength of heparin binding was primarily dictated by the C-terminal, spatially aligned lysine residues in the monomer state. The present study concludes that, under physiologic conditions, LA-PF4 monomers are highly preferred over dimers and tetramers; therefore, weaker heparin binding to LA-PF4 is at least partly the result of monomer preference in LA-PF4. This would effectively reduce by a factor of 4 the number of basic residues that define a protein-binding unit available for heparin interaction. Although the molecular nature of heparin–protein interactions is not well understood, positively charged amino acid residues are recognized as being necessary components for heparin binding. If we assume, as a first approximation, that the number of positive charges primarily determines anionic heparin binding, then, relative to PF4, LA-PF4 should elute from heparin–agarose columns at about one-quarter the NaCl concentration. In fact, PF4 is eluted at about 1.4 M NaCl and LA-PF4 is eluted at about 0.3–0.4 M NaCl (Rucinski et al., 1979; Holt et al., 1986), the difference being a factor of about 4. The charge difference between PF4 and LA-PF4 heparin-binding units, i.e., tetramer versus monomer, respectively, could by itself account for differences in the strength of heparin binding. It might even be suggested that low-affinity PF4 is a misnomer for LA-PF4 since many proteins probably interact with heparin just as weakly. A more appropriate name for LA-PF4 due to its high p*I* value of 8.0 is des(1–9) platelet basic protein after Holt et al. (1986). β-Thromboglobulin, likewise, should be named des(1–13) platelet basic protein. This is logical since all three proteins are immunologically and sequentially (excluding some N-terminal residues as cleavage products) identical. Doing this would avoid terminological confusion that presently exists in the literature in this field.

On the basis of sequence similarity, LA-PF4 and PF4 belong to a family of proteins involved in the inflammation response and immune regulation. These include interleukin 8 (IL-8)

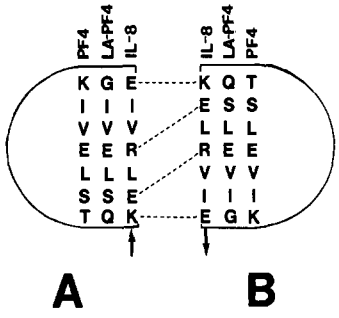

FIGURE 11: AB dimer interface domain for IL-8, LA-PF4, and PF4. Amino acid residues involved or thought to be involved (in the case of human LA-PF4 and human PF4) in the antiparallel β-sheet, AB-type dimer interface in bovine PF4 (St. Charles et al., 1989) and IL-8 (Clore et al., 1990) are shown schematically. Amino acid sequences are listed for residues in human LA-PF4, human PF4, and human IL-8.

(Larsen et al., 1989, and references therein), growth-related protein (Gro) (Anisowicz et al., 1987), Rous sarcoma virus-induced protein (9-E3) (Sugano et al., 1987), and interferon-induced protein (IP-10) (Luster et al., 1985). Also on the basis of conserved sequences and the relative, totally conserved location of four cystine residues, it has been suggested in several studies that monomer peptide folds in proteins of this family are similar. Presently, structural data on bovine PF4 (residues 24–85) from X-ray diffraction analysis (St. Charles et al., 1989) and on IL-8 from NMR structure analysis (Clore et al., 1990) support this hypothesis. The present NMR study indicates that, under physiologic solution conditions, LA-PF4 monomers and PF4 tetramers constitute biologically active states. Although working at pH 5.2 and apparently at low ionic strength, Clore et al. (1989) correctly invoke the presence of IL-8 dimers in order to explain their NMR structural data. IL-8 dimer formation, in itself, is perhaps not too surprising. What is interesting, however, is the comparison with bovine PF4. In the context of the bovine PF4 quaternary structure (St. Charles et al., 1989), IL-8 forms AB-type dimers. In both PF4 (Mayo & Chen, 1989) and LA-PF4 in this present study, AC-type dimers were found to be thermodynamically more highly favored in solution at low ionic strength. This can be understood when one considers the specific intersubunit, antiparallel β-sheet interactions in the AB-type dimer binding domains as shown in Figure 11 for PF4, LA-PF4, and IL-8. For this analysis, all three are assumed to form intersubunit, antiparallel β-sheet structures between AB-type dimers. For LA-PF4 and PF4, residues within this domain are highly conserved; opposing glutamic acid residues discussed previously are present in both, and hydrophobic residues flank them on either side. For IL-8, however, although the antiparallel β-sheet structure is conserved, the situation is different. The number of positively and negatively charged groups in this domain is greatly increased. In fact, Clore et al. (1990) suggest the possibility of salt bridge formation between all charged residues in this domain as indicated by dashed lines in Figure 11. These interactions would greatly stabilize AB-type dimers by removing the LA-PF4/PF4 Glu–Glu charge repulsion and by adding four salt bridges. AB-type dimer IL-8, therefore, probably is the biologically active state.

CONCLUSIONS

Under near-physiologic conditions, i.e., pH 7 and 0.2 M NaCl, human LA-PF4 exists predominately in the monomer state, while sequentially homologous PF4 exists predominately in the tetramer state. A third member in this protein family, IL-8, is found in the dimer state. Since monomer backbone folds are generally conserved in bovine PF4 and human IL-8 and most likely among other members of this family, various subunit combinations and permutations that define their quaternary structures may dictate respective biological functions.

ACKNOWLEDGMENTS

Ms. Hong Ma is gratefully acknowledged for having done some of the line-shape fittings and for drawing some of the figures.

Registry No. LA-PF4, 69344-77-0; PF4, 37270-94-3; heparin, 9005-49-6; LA-PF4 (human platelet reduced), 85496-03-3.

REFERENCES

Anisowicz, A., Bardwell, L., & Sayer, R. (1987) *Proc. Natl. Acad. Sci. U.S.A. 87*, 7188–7192.

Aune, K. C., & Timasheff, S. N. (1971) *Biochemistry 10*, 1609–1617.

Aune, K. C., Goldsmith, L. C., & Timasheff, S. N. (1971) *Biochemistry 10*, 1617–1625.

Begg, G. S., Pepper, D. S., Chesterman, C. N., & Morgan, F. J. (1978) *Biochemistry 17*, 1739–1744.

Busch, C., Dawes, J., Pepper, D. W., & Wasteson, A. (1980) *Thromb. Res. 19*, 129–138.

Cardin, A. D., & Weintraub, H. J. R. (1989) *Arteriosclerosis 9*, 21–32.

Caster, C. W., Miller, J. W., & Walz, D. A. (1983) *Proc. Natl. Acad. Sci. U.S.A. 80*, 765–769.

Clore, G. M., Appella, E., Yamada, M., Matsushima, K., & Gronenborn, A. M. (1989) *J. Biol. Chem. 264*, 18907–18911.

Clore, G. M., Appella, E., Yamada, M., Matsushima, K., & Gronenborn, A. M. (1990) *Biochemistry 29*, 1689–1696.

Cowan, S., Bakshi, E. N., Machin, K. J., & Isaacs, N. W. (1986) *Biochem. J. 234*, 485–488.

Denton, J., Lane, D. A., Thunberg, L., Slater, A. M., & Lindhad, U. (1983) *Biochem. J. 209*, 455–460.

Handin, R. I., & Cohen, H. J. (1976) *J. Biol. Chem. 251*, 4273–4282.

Holt, J. C., & Niewiarowski, S. (1980) *Biochim. Biophys. Acta 632*, 284–289.

Holt, J. C., Harris, M. E., Holt, A., Lange, E., Henschen, A., & Niewiarowski, S. (1986) *Biochemistry 25*, 1988–1996.

Ibel, K., Poland, G. A., Baldwin, J. P., Pepper, D. S., Luscombe, M., & Holbrook, J. J. (1986) *Biochim. Biophys. Acta 870*, 58–63.

Jeener, J., Meier, B., Backman, P., & Ernst, R. R. (1979) *J. Chem. Phys. 71*, 4546–4550.

Larsen, C. G., Anderson, A. O., Appella, E., Oppenheim, J. J., & Matsushima, K. (1989) *Science 243*, 1461–1466.

Lawler, J. W. (1981) *Thromb. Res. 21*, 121–127.

Lehninger, A. L. (1978) in *Biochemistry*, Worth Publisher, New York.

Loscalzo, J., Melnick, B., & Handin, R. I. (1985) *Arch. Biochem. Biophys. 240*, 446–455.

Lowry, O. H., Rosbough, N. J., Fan, A. L., & Randall, R. J. (1951) *J. Biol. Chem. 193*, 265–270.

Luster, A. D., Unkeless, J. C., & Ravetch, J. F. (1985) *Nature 315*, 672–676.

Marcum, J. A., & Rosenberg, R. D. (1984) *Biochemistry 23*, 1730–1737.

Mayo, K. H., & Chen, M. J. (1989) *Biochemistry 28*, 9469–9478.

Moore, S., & Pepper, D. S. (1976) in *Platelets in Biology and Pathology* (Gordon, J. L., Ed.) Vol. 1, pp 293–311, Elsevier, New York.

Moore, S., Pepper, D. S., & Cash, J. D. (1975) *Biochim. Biophys. Acta 379*, 379-384.
Mullenbach, G. T., Tabrizi, A., Blacher, R. W., & Heimer, K. (1986) *J. Biol. Chem. 261*, 719-722.
Mustard, J. F., Perry, D. W., Ardlie, N. G., & Packham, M. A. (1972) *Br. J. Haematol. 22*, 193-204.
Niewiarowski, S., Walz, D. A., James, P., Rucinski, B., & Keuppers, F. (1980) *Blood 55*, 453-456.
Patel, D. J., Woodward, C. K., & Bovey, F. A. (1972) *Proc. Natl. Acad. Sci. U.S.A. 69*, 599-602.
Paul, D., Niewiarowski, S., Varma, K. G., Rucinski, B., Rucker, S., & Lange, E. (1980) *Proc. Natl. Acad. Sci. U.S.A. 77*, 5914-5918.
Rao, A. K., Niewiarowski, S., James, P., Holt, J. C., Harris, M., Elfenbein, B., & Bastl, C. (1983) *Blood 61*, 1208-1214.
Rucinski, B. S., Niewiarowski, S., James, P., Walz, D. A., & Budzynski, A. Z. (1979) *Blood 53*, 47-62.
Schmid, J., & Weissman, C. (1987) *J. Immunol. 139*, 250-256.
Senior, R. M., Griffin, G. L., Huang, J. S., Walz, D. A., & Deuel, T. F. (1983) *J. Cell Biol. 96*, 382-385.
States, D. J., Haberkorn, R. A., & Ruben, D. J. (1982) *J. Magn. Reson. 48*, 286-293.
St. Charles, R., Walz, D. A., & Edwards, B. F. P. (1989) *J. Biol. Chem. 264*, 2092-2099.
Stern, D., Nawroth, P., Marcum, J., Handley, D., Kisiel, W., Rosenberg, R., & Stern, K. (1985) *J. Clin, Invest. 75*, 272-279.
Sugano, S., Stoeckle, M. Y., & Hanafusa, H. (1987) *Cell 49*, 321-328.
Waddell, W. J. (1956) *J. Lab. Clin. Med. 48*, 311-314.
Wüthrich, K. (1986) *NMR of Proteins and Nucleic Acids*, Wiley Inc., New York.
Wyman, J. (1964) *Adv. Protein Chem. 19*, 224-250.

Characterization of the Kinetic Pathway for Fibrin Promotion of α-Thrombin-Catalyzed Activation of Plasma Factor XIII†

Michael C. Naski,*,‡ Laszlo Lorand,§ and Jules A. Shafer‡

Department of Biological Chemistry, The University of Michigan, Ann Arbor, Michigan 48109, and Department of Biochemistry and Molecular and Cell Biology, Northwestern University, Evanston, Illinois 60201

Received July 24, 1990

ABSTRACT: Kinetic and thermodynamic studies are presented showing that the cofactor activity of fibrin I (polymerized des-A fibrinogen) in the α-thrombin-catalyzed proteolysis of activation peptide (AP) from plasma factor XIII can be attributed to formation of a fibrin I–plasma factor XIII complex (K_d = 65 nM), which is processed by α-thrombin more efficiently ($k_{cat}/K_m = 1.2 \times 10^7$ M^{-1} s^{-1}) than free, uncomplexed plasma factor XIII ($k_{cat}/K_m = 1.4 \times 10^5$ M^{-1} s^{-1}). The increase in the specificity constant (k_{cat}/K_m) is shown to be largely due to an increase in the apparent affinity of α-thrombin for the complex of plasma factor XIII and fibrin I, as reflected by the 30-fold decrease in the Michaelis constant observed for fibrin I bound plasma factor XIII relative to that for uncomplexed plasma factor XIII. Analysis of the initial rates of α-thrombin-catalyzed hydrolysis of fibrinopeptide B (FPB) from fibrin I polymer in the presence of plasma factor XIII indicated that α-thrombin bound to fibrin I in the ternary complex of α-thrombin, plasma factor XIII, and fibrin I polymer is competent to catalyze cleavage of both FPB from fibrin I and AP from plasma factor XIII. This observation is consistent with the view that α-thrombin within the ternary complex is anchored to fibrin I polymer through a binding site distinct from the active site (an exosite) and that the active site is alternatively complexed with the AP moiety of plasma factor XIII or the FPB moiety of fibrin I. This conclusion is supported by the observation that a 12-residue peptide, which binds to an exosite of α-thrombin and blocks the interaction of α-thrombin with fibrinogen and fibrin, competitively inhibits α-thrombin-catalyzed release of both FPB and AP from the fibrin I–plasma factor XIII complex.

In the final step of the blood coagulation cascade, the transglutaminase $FXIII_a$ catalyzes formation of γ-glutamyl-ε-lysyl peptide cross-links between adjacent fibrin units of the blood clot [for a review, see Lorand et al. (1980)]. These cross-links increase the mechanical strength of the blood clot (Roberts et al., 1974; Gerth et al., 1974). $FXIII_a$ also catalyzes the cross-linking of α_2-antiplasmin to fibrin, thereby increasing the resistance of the clot to dissolution by plasmin and increasing the lifetime of the clot in plasma (Sakata & Aoki, 1980, 1982; Jansen et al., 1987).

Scheme I

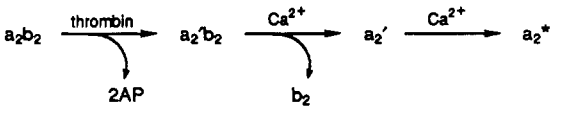

Plasma factor XIII circulates in blood plasma as a zymogen composed of two a subunits and two b subunits. Activation of plasma factor XIII is accomplished by the successive actions of α-thrombin and calcium as shown in Scheme I, wherein α-thrombin catalyzes cleavage of a 37-residue activation peptide (AP)[1] from the N-terminus of each of the a subunits

† This study was supported by National Institutes of Health Grants HL 026345 (to J.A.S.) and HL 02212 (to L.L.), U.S. Public Health Service Research Career Award HL 03512 (to L.L.), and a Horace H. Rackham Predoctoral Fellowship (to M.C.N.). Part of this work is taken from a Ph.D. thesis to be submitted by M.C.N. to the Graduate School of The University of Michigan.

‡ The University of Michigan.
§ Northwestern University.

0006-2960/91/0430-934$02.50/0